

**The Effects of Near-Vacuum Solar Irradiation on the Morphology and Growth Kinetics of
Arthrospira Platensis and *Chlorella Vulgaris***

NASA Colorado Space Grant Consortium DemoSat B Summer 2021



From left to right: Justin Raffa, Karla Rueda Perez, Richard Nash, Jacob Julius

Jacob Julius, Richard Nash, Karla Rueda Perez, Justin Raffa

Colorado State University

Team Algae Sous Vide Dotées UV

8/14/2021

Graduate Advisor: James Sipich
CSU NASA Space Grant Program Director: Dr. Azer Yalin

Abstract

In recent years, multiple aerospace communities have begun investigating the potential usefulness of microalgae as a means of facilitating human travel deeper into space. Microalgae possess a unique set of traits that make them a promising solution for long term space travel and extraterrestrial colonization. They are currently being studied on the International Space Station to investigate the viability of supplementing life support systems via conversion of CO₂ to O₂ during photosynthesis [1]. They can provide a sustainable and nutrient dense food source to astronauts to cut down on the overall weight of sustenance required at journey's onset [1]. They can synthesize bioethanol through exposure to a fermentation process [2]. Biodiesel can also be harvested from the high lipid contents of some strains, potentially making them a sustainable fuel source for extraterrestrial bases [2]. They can even assist in the downstream stages of wastewater treatment by removing excess nitrate and phosphorus from the stream [3]. If algae are to accompany humans deeper into space, further from the robust supply chains needed to sustain us there, the value in understanding how these organisms respond when exposed to increased levels of cosmic radiation experienced in space becomes apparent. This report documents an attempt to gather such data utilizing the stratospheric flight capabilities of a high altitude weather balloon to simulate near space solar radiation conditions for the algae species *Chlorella Vulgaris* (CV) and *Arthrospira Platensis* (AP).

Table of Contents

Abstract	2
Introduction	5
Mission Overview	5
Experimental Design	5
Mission Importance	5
Phycology	6
Goals and Methods	6
Standard Operating Procedures	7
Arthrospira Platensis	7
Morphology	7
Applications	8
Chlorella Vulgaris	8
Morphology	8
Applications	9
Hypothesized interactions between UVC radiation and organelles/DNA	9
Payload Design	10
Goals	10
Systems	10
Structural	10
Electrical	12
Preliminary Testing	12
Algae	12
Quantifying UVC Irradiance	12
Mother Cultures	13
Algae Pre-Flight Trials	14
Material Viability Calculations	16
Structural	17
Predicting Internal Pressure	18
Window Transmissibility	21
Electronics	22
Heat Transfer	22

Flight Day	23
Data and Observations	24
Observations	24
Sensor Data	25
Algae Data	26
Temperature and pH	27
Biomass	27
Microscopy Preflight	27
Microscopy Postflight	28
Budget, Management, and Schedule	30
Management	30
Schedule	30
Financial and Mass Budgets	30
Conclusions	31
Message to Next Year	31
Acknowledgments	32
References	32

1) Introduction

Humanity's exploratory nature has fueled an ever present fascination with what lies beyond Earth's atmosphere. The more we understand our solar system, the more we yearn to go to these places that are currently the domain of unmanned probes and surface rovers. The Apollo missions of the 60s and 70s represent the peak achievements of human space exploration efforts thus far. As interest grows in extending human reach past the lunar surface, extensive planning and research is required in order to identify working, habitable solutions for humans in deep space flight. An intriguing area of this research is the investigation into utilizing microalgae to facilitate human exploration of deep space.

These organisms show potential as a means of supplementing currently existing life support systems by increasing their ability to generate breathable oxygen and remove carbon dioxide from the living environment [4]. This concept is currently being investigated on the International Space Station (ISS), and initial reports seem to show promise [1]. Algal biomass can be harvested and used as a replenishable food source. Additionally, multiple processes are being developed and refined that allow these organisms to be used in the synthesis of ethanol and diesel fuel [2]. All these capabilities within one subset of microscopic organisms make microalgae an intriguing prospect as an enabler of human deep space exploration

and/or colonization. To that end, increasing our understanding of how these organisms may react when removed from their native environments here on Earth is an important step in developing our capabilities for taking them deeper into space.

2) Mission Overview

Experimental Design

A payload was designed for stratospheric flight on a high-altitude weather balloon. The goal of the experiment was to utilize the balloon to lift the payload above an altitude where significant atmospheric scattering of light occurs in order to allow for more harmful wavelengths of cosmic radiation to irradiate samples of microalgae (species *Chlorella Vulgaris* and *Arthrospira Platensis*) in near space conditions [5].

Mission Importance

Although technology to irradiate algae is available on Earth's surface, utilizing the weather balloon to achieve this UVC exposure in the upper atmosphere provides a much cheaper, less complex method of achieving near space conditions. To achieve this in a traditional laboratory setting, researchers must attempt to simulate solar spectra distribution and intensity of specific wavelengths. Near space conditions also incorporate far lower

temperatures and pressures than are possible on the ground without expensive equipment and high energy costs. The balloons allow for easy replication of near space conditions with less technical design considerations, lower energy cost, and few additional considerations (like ensuring the payload survives its flight, issues with where it may land, etc.).

3) Phycology

Goals and Methods

Experimentation on algal cultures was performed for the purpose of identifying optimal growth conditions and studying the effects of different stimuli on growth kinetics and morphology. These effects directly impact the cell quantity and thus the ability for the algae to perform their tasks such as gas conversion and biomass food yield. Optical density, biomass, and microscopy tests were performed to observe stimuli effects and quantify growth while light exposure, pH, temperature, and aeration were compared to growth rates to analyze the growth environment. pH was observed through paper pH strips.

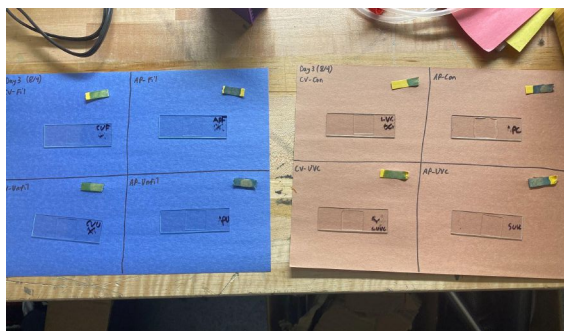


Fig. 3.1: pH strips and microscope slides



Fig. 3.2: Temperature was taken by a meat thermometer and recorded in °C.

Nominal light exposure and aeration were investigated from literature. Biomass was obtained by drying a set volume of culture on filter papers and converted to concentration by dividing dry cell mass by the volume of culture used.



Fig. 3.3: Biomass testing

Optical density was measured with the Secchi stick method and converted to concentration via a mathematical model that compared secchi depth to the

concentration values gained from the biomass test. The Secchi stick is a simple analytical instrument used to measure a liquid's turbidity. The instrument has a target on the bottom of a ruler. When the stick is lowered, the depth at which the target disappears is the Secchi depth. This can be correlated to the relative concentration of particulate matter present in solution, assuming perfect mixing.



Fig. 3.4: Optical density test

Standard Operating Procedures

Standard operating procedures (SOPs) were developed to reduce experimental error, prepare for post flight inoculations, ensure lab sterility, and allow for experiment replication. These procedures include: mother culture inoculations, test inoculations, flight day inoculations, testing procedures (optical density, pH, temperature, biomass, microscopy, and macroscopic observations), contingency plan for if the samples were frozen upon retrieval, and harvesting to prevent overcrowding of biomass in the culture.

Arthrospira Platensis

Morphology

Arthrospira Platensis (AP), commonly known as Spirulina, is a filamentous, extremophilic cyanobacteria that assumes a characteristic helical orientation, called a trichome (see Fig. 3.5) [6].

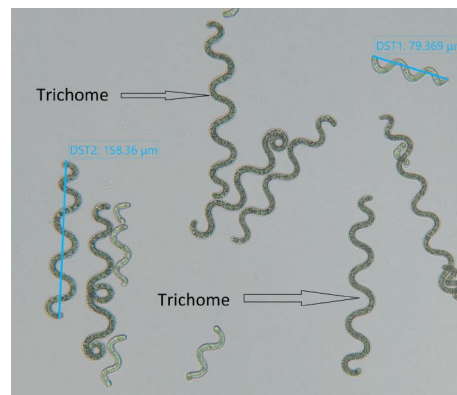


Fig. 3.5: AP trichomes

AP reproduces asexually via hormogonia differentiation. Hormogonia differentiation results from trichome fragmentation (see Fig. 3.6) [6],[7].

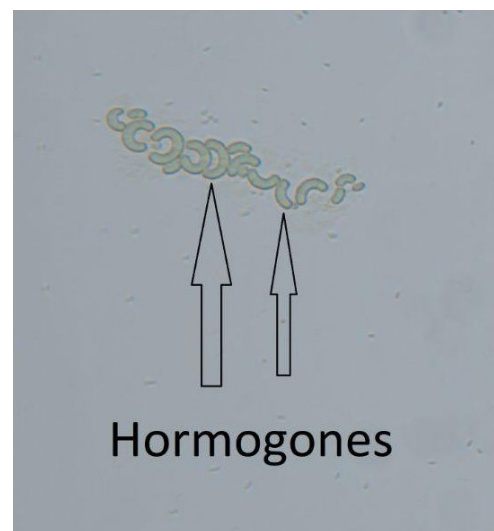


Fig. 3.6: Hormogones: sections of the original trichome

Phycocyanin, a blue phycobiliprotein, is the primary photosynthetic pigment of AP [6]. Chlorophyll *a* and *b* are also present, albeit in lesser concentration [6]. These pigments are the cause of the dark blue-green color in AP cultures as seen in figure 3.7.

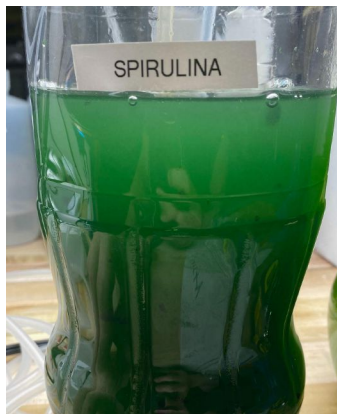


Fig. 3.7: Typical AP Culture Color shown in α -variant mother culture

Applications

This species is in the photosynthesizing *Cyanophyceae* class that was critical for the development of aerobic life forms during the Great Oxidation Event in the early history of Earth [6],[7]. Cyanobacteria have a higher photosynthetic efficiency than most plant life which allows for enhanced gas transfer and faster growth [8]. AP is nutrient dense, containing essential micronutrients such as calcium, iron, magnesium, potassium, and vitamins C, B-6, A, and K [9]. Furthermore, AP has more protein per gram than steak (0.58 g as opposed to 0.31 g, respectively) [9]. AP is thus an intriguing candidate for air recycling and sustainable food supplements during long

space flights or extraterrestrial colonization. Due to a low lipid content, AP is not a good candidate for biofuel production. However, AP can be used to treat wastewater [8].

Chlorella Vulgaris

Morphology

Chlorella Vulgaris (CV) is a spherical, eukaryotic green algae that belongs to the phylum *Chlorophyta* [6]. CV contains the primary pigments chlorophyll *a* and *b* which result in its light green color [10]. Reproduction is asexual via multiple fission (see Fig. 3.8) in which mature cells can produce more than 2 daughter cells as in binary fission [11]. The offspring are always in multiples of 2, however, and it was found that groups of 4 were most common in this experiment's CV [11].

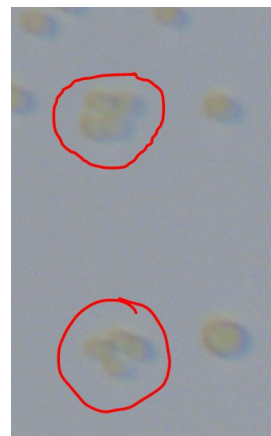


Fig. 3.8: Multiple fission quadruplets

CV tends to aggregate in vitro. These aggregates, called flocculations, were found to be especially prevalent in nutrient deficient cultures and could be dispersed

by perturbing the culture via mechanical mixing (see Fig. 3.9).

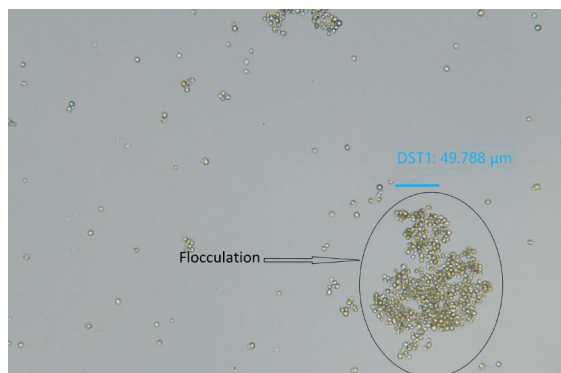


Fig. 3.9: CV flocculation

Applications

CV is one of the most studied species of microalgae for its ability to treat wastewater as well as its high efficiency in photosynthesis and biofuel production [12]. Treating wastewater is a complicated process in which macromolecules such as nitrates and phosphorus must be removed, as well as trace metals such as cadmium and chromium. While most algal species consume the macromolecules in wastewater, the trace metals that are uptaken are species dependent and thus a series of bioreactors containing different algal species is likely required [3]. CV will specifically uptake cadmium, copper, and zinc [3]. CV has an abnormally high lipid content, 20%-32%, which makes it more effective as a source of biodiesel [12].

Hypothesized interactions between UVC radiation and organelles/DNA

It is generally accepted in the scientific community that high energy radiation, such

as UVC and X rays, will denature proteins [5]. Based on this it was hypothesized that the algae cultures would be decimated by the destruction of their primary photosynthetic pigments as well as other necessary protein structures. Ionizing radiation tends to create free radicals in the cell by inducing high energy quantum states in electrons, leading to electron displacement [5], [13]. These radicals can cause localized damage to cellular structures due to their increased chemical reactivity [14]. UVC radiation can cause double strand breaks in both nuclear and extranuclear DNA [14]. Mutations may occur through the improper repair of these double strand breaks [14]. It was hypothesized that these mutations would propagate through the system as the algae reproduced and become more evident with time.

A study from *NCBI.gov* found that UVC was extremely effective at eliminating bacteria and fungi:

“The calculated irradiance at the device aperture was 15.54 mW/cm², with the distance between the UVC lamp and suspension surface 25.4 mm. Upon exposure to UVC, a 99.9% inactivation rate was obtained at 3–5 s for the bacteria (*P. aeruginosa* and *Mycobacterium abscessus*) tested. By contrast, 15–30 s of UVC treatment was required to obtain 99.9% inactivation of the fungi (*Candida albicans*, *Aspergillus fumigatus*) tested” [14].

This statistic is likely applicable to microalgae, whose sizes are on the same order of magnitude as bacteria and fungi.

4) Payload Design



Fig. 4.1: The payload (featuring Phil)

Goals

The primary goal of the experiment was to allow for the high-altitude solar irradiation of four samples of algae in order to gather data about how algae responds to conditions it may experience during deep space exploration. The samples were to be kept in a liquid medium and thus it was hypothesized early on in the design phase that the algae needed to remain at atmospheric pressure in order to cut down on the amount of variables in the experiment, as well as to prevent the off-gassing of valuable nitrogen from the sample containers [15], [6]. To this end, the structural materials of the payload were chosen with an expectation that they would need to both provide a seal and be able to hold up structurally under the stress forces produced by the difference in internal and external payload pressure.

Systems

Structural

Braided carbon fiber tubing was selected for its low weight and ability to withstand stress forces from the pressure gradient that would develop during flight in the event of a successful seal [16]. This material was certainly capable of containing the internal pressure from a force perspective, however a ‘natural’ finish was selected to save money. Upon arrival, this ‘natural’ finish was deemed incapable of holding a seal; multiple holes were visible on the inside of the tube’s epoxy finish. In retrospect, the better decision may well have been to spend the extra \$30.00 or so to get a ‘gloss’ finish to facilitate the sealing of the structure. In the initial stages of development, extra epoxy was applied to the insides of the tubes in an attempt to plug any potential holes.

The end caps for the design were to be printed with polyethylene terephthalate glycol (PETG) 3D printing filament and epoxied to the tubing. PETG was selected for its low price and improved material qualities over other similarly cheap filament options like Polylactic Acid (PLA) or Acrylonitrile Butadiene Styrene (ABS) [17], [18], [19]. PLA proved too brittle when cursory shock and force testing was conducted (some old PLA & PETG prints were gathered and slammed to the floor). ABS is difficult to print with and also has increased safety considerations due to vaporous emissions during printing [19]. It was decided that

PETG provided a decent balance between structural rigidity and brittleness, was lightweight enough to include on the payload, cheap enough to keep a steady amount on hand, and it could be treated post print to achieve any additional requirements. Some downsides to this decision were discovered later in the project when structural and pressure testing began. Even with relatively high detailed settings placed into the printers, the plastic allowed air to pass straight through it even with minimal pressure gradients present. This significantly complicated efforts to seal the payload during scale up from smaller prototypes.

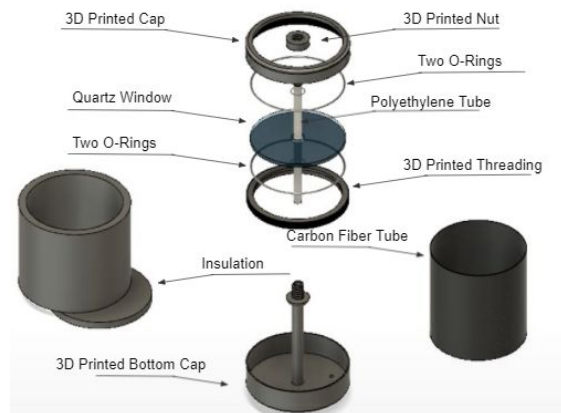


Fig. 4.2: Exploded view of payload design

Fused quartz was selected for the window material as a balance between price and deep UV wavelength transmissibility (about 70% transmissibility at 220 nm, 30% at 200 nm) [20]. Options exist that transmit deeper into the UVC area of the electromagnetic spectrum (like fused silica, or sapphire glass) [20]. However, samples of these large enough for the window in the original design idea proved to be prohibitively expensive. This original idea

was eventually scrapped for a dual semicircular design in order to simplify the cutting process of the window and to cut weight.

The payload was externally padded with three layers of aluminum-lined polyethylene (PE) insulation often used in HVAC systems. One layer of this insulation was also applied to the inner walls of the payload, as well as around the central column of the design.

The internal structure of the payload consisted of a cardboard platform, plastic inner column to slide over the central column, cardboard slabs to contain the electronics and battery, and an acrylic platform lined with insulation to support the biological samples below the window.

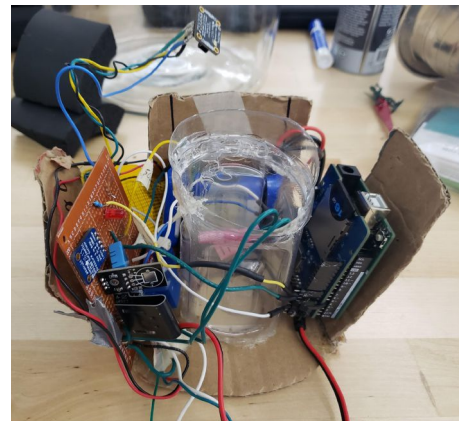


Fig. 4.3: Internal electronic boards

Electrical

An Arduino UNO was used to control the electronics needed for the payload. It's first job was to monitor the temperature from a DHT11 temperature and humidity sensor. The heaters were connected into the

Arduino through a relay, and the Arduino was programmed to operate the relay if the temperature ever dropped below 15 °C. During initial testing, 12V of potential proved to be more effective at heating the payload rather than the 5V supplied by the Arduino. The decision to use a single 12V battery to supply power to the system necessitated a voltage regulator to step down the voltage to 5V, to protect the Arduino. The battery was split in parallel between the relay and the voltage regulator to keep a full 12V going to both circuits. This allowed the Arduino to be run on 5V while the heaters ran on their more efficient 12V circuit, from the same power source, without frying the microcontroller. The Arduino's second task was to record all the data from the sensors to an SD card. The sensor array included a DHT11 (temperature/humidity), a BMP180 (pressure/temperature), and a TSL2591 (illuminance of infrared & visible light / total lux). The SD card also recorded a time in seconds at the end of every loop. This was a simple way to get the relative duration the Arduino was running.

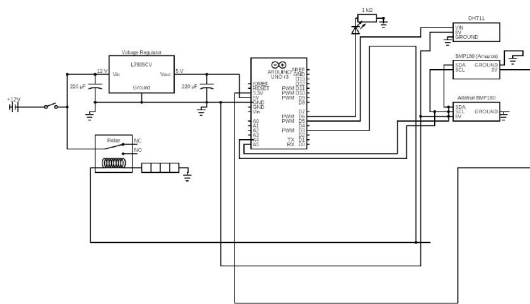


Fig. 4.4: Wiring diagram of electronics

5) Preliminary Testing

Algae

Quantifying UVC Irradiance

A mathematical model was developed to translate the readings from the radiation sensors into a solar spectra distribution that could yield the radiative intensity for the wavelength ranges being analyzed. The model was simplified by assuming the sun to be a perfect blackbody emitter at a constant 5778 K temperature and an even distribution of atmospheric photon scattering across all electromagnetic wavelengths. The model begins by inputting the parameters of absolute temperature of the sun (5778 K) and a large vector of wavelength values into two Planck's law functions [13].

$$B_{\lambda}(T) = \frac{2hc^2}{\lambda^5} \frac{1}{e^{\frac{hc}{\lambda kT}} - 1}$$

Fig 5.1: Planck's law

The first equation yields the blackbody distribution for the entire electromagnetic spectrum by utilizing a vector from 1 nm to 1 m with 100,000,000 evenly spaced points. The second equation yields the UVC region of the EM spectrum by utilizing a vector from 100 to 280 nm with 100,000,000 evenly spaced points. A ratio of the integrals of these two distributions, demonstrated in figure 5.2, can be then multiplied by the solar intensity found by the TSL2591 sensor to yield the total

exposure to UVC radiation. 1350 W/m^2 , the sun's irradiance in vacuum, was used as a baseline and resulted in 150.045 W/m^2 of expected UVC radiation under ideal conditions.

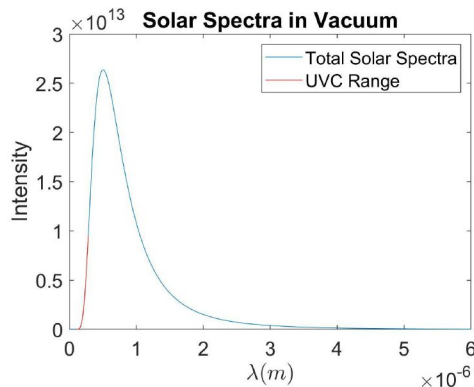


Fig. 5.2: Solar spectra in vacuum

One issue, however, is that the TSL2591 sensor outputs values in lux (lumens/m²) rather than W/m². These lux values can be converted to W/m² by dividing the lux value by the mean luminous efficacy for direct sunlight, which is 105 lumens/W at high elevation [21]. This procedure was used to attempt to quantify the total UVC exposure of the samples during their flight.

Mother Cultures

Large volume ‘Mother cultures’ were inoculated for the purpose of having a sustainable source of algae for testing and flight day. The cultures were grown at room temperature with aquarium aerators and 30W bright white shop lights (Fig. 5.3).



Fig. 5.3: Mother cultures

The cultures followed a cycle of growth → dilution → growth → harvest → dilution. The cultures were diluted periodically and harvested when the Secchi depth was between 10mm and 20mm. Generally, these cultures grew quickly and were healthy. However, both AP mother cultures became infected with multiple species of bio-contaminants nearing flight day. This led to the death of the cultures (Fig. 5.4). These bio-contaminants ranged from ‘worm-like’ parasites to grazers that eat algae cells. These grazers were not hypothesized to be microzooplankton, which are one of the largest issues in industrialization of algae, but rather of the genus *Petalomonas* due to their flagellated, colorless appearance and phagotrophic tendencies (Fig. 5.5) [22].



Fig. 5.4: Healthy CV culture (left) and dead AP culture (right)



Fig. 5.5: AP biocontaminants

The AP cultures were replaced 5 days before flight day. This was unfortunate since the cultures were likely still in the lag phase of growth on flight day.

Algae Pre-Flight Trials

Four pre-flight algae “trials” were conducted to observe the effects of nutrient/salt concentration, vacuum, and cold vacuum on growth and morphology. The first two trials measured growth using the original media recipes from Algae Research and Supply (AP: 15g alkali salts,

2mL liquid nutrients, 1L DI H₂O CV: 2g freshwater salts, 1mL liquid nutrients, 1L DI H₂O). This experiment used 40mL of media to 10mL of algae ‘seed’. The second trial indirectly changed the salt and nutrient concentration by increasing the media to algae seed ratio to 42mL media: 8mL algae seed. In the third and fourth trials, the 8mL algae seeds were injected into plastic test tubes and exposed to vacuum. In these trials the algae was subjected to -24.5 inHg of vacuum (≈ 0.02 atm) for 2 Hours. Trial 3 was kept at room temperature while trial 4 was placed in an ice water bath.

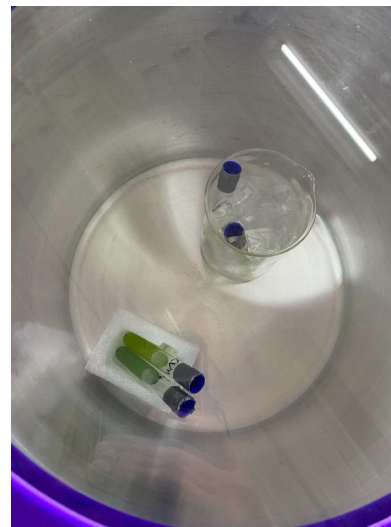


Fig. 5.6: Vacuum trials

It was found that the vacuum would cause the liquid to undergo desorption and a large fraction of the seed would be lost to the vacuum chamber due to violent bumping. This issue was solved by cutting a hole in the test tube cap and covering it with an air permeable, waterproof membrane, such as neoprene. Using this strategy, the effects of vacuum on the algae could be observed

and the original 8mL of seed would be retained.

It was found that the second trial (42mL media: 8mL seed) showed slightly better growth than trial 1 (40mL media: 8mL seed) and thus this ratio was used for subsequent trials and for the flight. As predicted, the vacuum trials showed decreased growth and significant structural damage as depicted in figures 5.7 and 5.8.

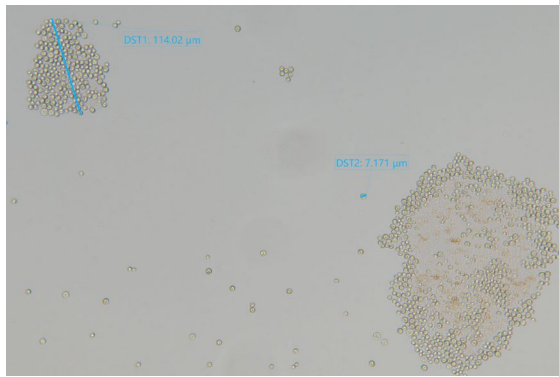


Fig. 5.7: CV trial 4

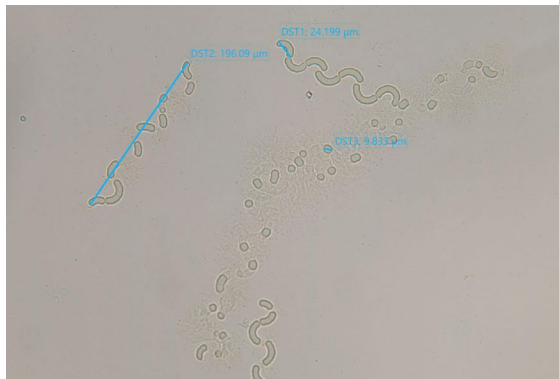


Fig. 5.8: AP trial 3

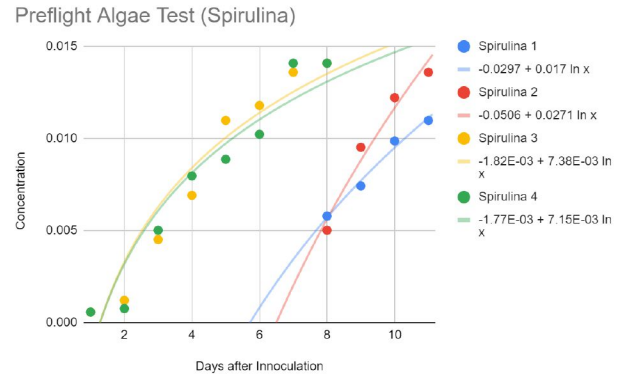


Fig. 5.9: Quantifying AP Growth

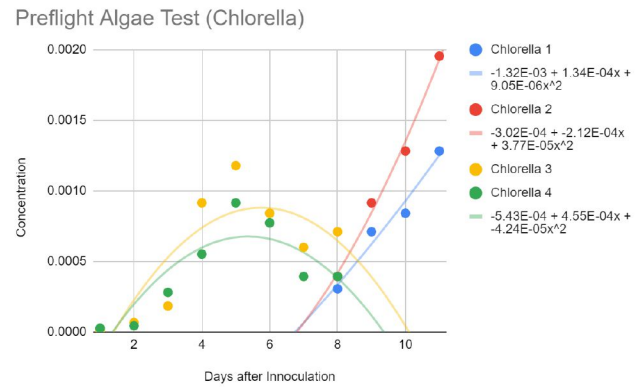


Fig. 5.10: Quantifying CV Growth

Material Viability Calculations

To test the material considerations before ordering parts, some calculations were developed to test their properties. The tensile strength of both the carbon fiber and fused quartz were compared to the maximum pressure force the payload would experience [16], [20]. Maximum pressure forces were calculated by multiplying the atmospheric pressure at the altitude where the payload would be sealed by the internal surface area of the payload. Both materials were determined to be strong enough for the maximum expected force. A safety factor was also calculated

for the window. According to Advance Glass Industries, the safety factor needed to be between 4-7 and the calculated value was 7.0 [23].

Carbon Fiber Thin Wall Pressure

Hoop Stress

$$\sigma_{\theta} = \frac{PD_o}{2t}$$

Mean Diameter, D_m = outside diameter - t = .1524m - 0.001998m = 0.1504m

Pressure, P = 85113Pa

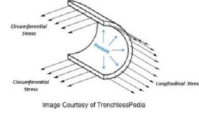
Thickness, t = 0.001998m

$$\sigma_{\theta} = \frac{PD_o}{2t} = \frac{(85113Pa)(0.1504m)}{2(0.001998m)} = 2990456.757Pa = \boxed{3.0MPa}$$

Longitudinal Stress

$$\sigma_L = \frac{PD_o}{4t} = \frac{(85113Pa)(0.1504m)}{4(0.001998m)} = \boxed{1.5MPa}$$

Tensile Strength of Carbon Fiber = **228GPa**



Fused Quartz Pressurized Window

Maximum Stress

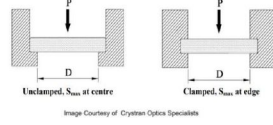
Empirical Constant, k = 1.125(Unclamped)

Unsecured Diameter, D = 0.127m

Pressure, P = 85113Pa

Thickness, t = 0.00635m

Flexural Strength, F_u = 67MPa



$$S_{max} = \frac{(kD^2P)}{4t^2} = \frac{1.125(0.127m)^2(85113Pa)}{4(0.00635m)^2} = 9575212.5Pa = \boxed{9.6MPa}$$

$$\text{Safety Factor} = \frac{F_u}{S_{max}} = \frac{67MPa}{9.6MPa} = \boxed{7.0}$$

Fig. 5.11: Force calculations

Another consideration was thermal expansion/contraction. Since a net decrease in temperature was expected as altitude increases, thermal contraction was considered. Using the coefficient of thermal expansion for the chosen materials and a temp of -80°C, an approximate worst case scenario for material shrinkage was calculated [20], [24], [25]. The interfacing of three different materials in the payload design led to concerns about some items shrinking more than others causing tiny cracks through which air could leak or even compromise the overall external payload structure. The thermal expansion coefficient of carbon fiber was found to be negligible so shrinkage was only calculated for fused quartz and PETG [20], [24], [25]. The largest change seen was 0.068mm, so thermal compression was also deemed negligible with the materials chosen.

Coefficients of Thermal Expansion

ΔL = Change in length, α = Coefficient of thermal expansion, L = length, and ΔT = change in temperature

$$\Delta L = \alpha L \Delta T$$

- Fused Quartz

$$\begin{aligned} \alpha &= 5.5 \times 10^{-7} \frac{1}{K} \\ L &= \frac{1}{4} = 6.4 \times 10^{-4}m \\ \Delta T &= (20C - -80C) = 100K \\ \Delta L &= 6.8 \times 10^{-5}m = 0.068mm \end{aligned} \quad (1)$$

- PETG

$$\begin{aligned} \alpha &= 6.8 \times 10^{-5} \frac{1}{K} \\ L &= \frac{1}{4} = 0.0064m \\ \Delta T &= (20C - -80C) = 100K \\ \Delta L &= 4.318 \times 10^{-5}m = 0.043mm \end{aligned} \quad (2)$$

Fig. 5.12: Thermal expansion calculations

Structural

The payload was constructed so force testing could begin. The payload was dropped off the roof at a height of 15 feet. When it was dropped it hit a small awning on the side of the wall, sending the payload into a spiral. It landed on the corner and bounced. The test was photographed rapidly to allow for an in depth review of the results. From the pictures, the window broke on the initial impact with the ground. The central column broke at the top nut, and the glass had a radial break around the hole in the center. It was hypothesized that the impact forces absorbed by the payload caused instantaneous deformation of the payload structure, causing the central column to essentially ‘punch through’ the weak point at the center of the glass. From this test, it was concluded that two layers of insulation were not sufficient to absorb the expected impact forces possible during landing.



Fig. 5.13: Radial glass shatter in the first drop test

Two upgrades were integrated into the payload. Instead of a full piece of glass across the whole top. Two semi circular pieces were used instead. This eliminated the need to drill a hole in the glass, which decreased its overall structural integrity. Instead of directly contacting the glass window, the central column was in contact with a thin ‘bridge’ of PETG that ran across the top of the cap and between the two semi-circular windows. In the case of a high-velocity impact, the deformation would cause the column to hit the PETG and not the glass. To help the overall payload with impact, force dampeners were added to the outside of the payload. These force dampeners hit the ground first to absorb most of the impact force. The material chosen for this was a thick pipe foam insulation. The aluminum lined insulation used for keeping the heat was very stiff and didn’t compress well, however this pipe foam was much thicker, compressible, and was found to absorb impact well.



Fig. 5.14: The white arrows point to the force dampener upgrades

With these new upgrades the payload was ready to test again. The payload was dropped from 15 feet again with no damage to the window or the internals. The force dampeners worked as designed. With a successful drop test, the payload was then subjected to the stair test with no issues.

Predicting Internal Pressure

To test the viability of pressurising the payload, smaller prototypes were developed. Each tube was a 3 inch carbon fiber tube with PETG printed end caps, where one side screws open.



Fig. 5.15: From left to right; Bike Pump test, JB Weld full coating, Potted JB Weld, Rubber inner lining, PVC inner lining and control

The first test was the bike pump test to confirm whether the chosen materials

would indeed stand up to the expected pressure forces. Two end caps were epoxied to the ends of a carbon fiber tube. One side had a hole drilled in it and a Schrader bike tire valve stem attached. The goal of this prototype was to test carbon fiber to PETG adhesion strength as well as its ability to hold pressure. With the valve on one side, a standard bike pump could be used to build pressure on the inside. Pressure was monitored using the gauge on the pump. To test whether it was airtight, the tube was pressured to ~15 psi, then submerged under water to identify any locations where bubbles may have been formed. The test showed that air was flowing directly through the cap and not through a crack or any specific part of the print. It was also observed that no bubbles came out of the pump side, the carbon fiber tubing or any of our epoxy seams. It is hypothesized that the excess rubber around the Schrader valve also got sealed into the epoxy on that side, stopping the airflow. This test was then repeated after an application of aerosol Flex Seal rubber coating to see if a post-process sealant could solve the sealant problems. After spraying multiple layers and retesting multiple times, there was a decrease in air bubbles coming through but still too many to call it a success. For one last test the tube was pumped to its maximum pressure to see if a rupture occurred. The adhesion between the carbon fiber and PETG maintained integrity all the way to 100 psi. This confirmed the ability of the chosen materials to contain the necessary pressure forces.



Fig. 5.16: Bike pump test setup.

Focus then turned to achieving a proper seal. Four more tubes were cut and matching end caps were printed with the goal of achieving a seal that would hold in vacuum. These prototypes each had screw on end caps, which was closer to the actual payload design. To quantify the data these tubes were placed into a vacuum chamber with a pressure sensor connected to an Arduino mini. A 433MHz transmitter would send internal pressure readings to another arduino board with an RF receiver outside the vacuum chamber. Vacuum was pulled in -5 inHg increments utilizing a 5 gallon vacuum chamber from Best Value Vacs and an IDP2 vacuum pump from Varian. Tubes 1 and 2 were adhered using JB Weld. Tube 1 was tested with a technique called potting (using the vacuum chamber while the epoxy cures to pull out air bubbles). Tube 2 was tested with the same JB Weld epoxy but without potting. Tube 1 performed poorly. With only -5 inches of mercury the internal and external pressures equalized almost instantly. This is likely due to the wet epoxy vacuum curing process. The hypothesis is that during our attempt to ‘de-gas’ the epoxy resin with vacuum, the bubbles that were pulled formed ‘channels’ in the external

resin seal that allowed for the free flow of air upon curing. This likely occurred due to the highly viscous nature of JB Weld original steel reinforced epoxy in its liquid state. Tube 2 performed better. The tube did leak pressure, about 2 kpa every couple seconds. However, the rate of pressure change stayed constant even to maximum vacuum (-25 inHg). By the time the chamber reached maximum vacuum, the internal pressure had only dropped from 850 to 650 kpa.



Fig. 5.17: Test 1- vacuumed JB Weld (left) and Test 2- regular cured JB Weld (right)

To build upon the results seen from the last two tests, three more prototypes were developed. A threaded sleeve similar to the full sized design was printed with slots for a smaller O ring and was used on all subsequent prototype testing. The first had a full coat of JB Weld applied to the outside of the tube. The second had a layer of rubber to line the inside of the prototype, essentially forming a gasket along the entire internal surface area of the prototype. The third used a PVC liner to save weight from the heavy rubber liner. Both the JB Weld and the rubber liner tubes performed better in the vacuum chamber than previous tests but still leaked. Liquid PTFE sealant was applied to the threads on both the full coat and the

rubber liner prototypes to attempt to stop any leak from the threads. This method slowed the leaks, however the required cure time for the PTFE sealant was 24hrs (too long to be practical to seal on the morning of flight). For most tests, 30 minutes of cure time was allotted for the PTFE to cure due to concerns about battery life for the internal pressure sensor module. The goal for a 'successful' prototype trial was changed from achieving a complete seal to minimizing the rate of leakage to an acceptable rate for a duration longer than any expected flight would take (~3.5-4 hrs). The half hour cure time slowed the leaking slightly, but the PTFE sealant was observed to bubble at the edge of the threads, indicating a leak through the threads (or the PETG itself). The most successful run involved the 'full coat' external epoxy tube, the non vacuum cured cap, a circular rubber gasket underneath the cap to address any issues with the O ring, and a very liberal application of PTFE thread sealant both on top of the O ring and in the threads. With this design, a leak rate of 0.001-0.002 kPa every 7 seconds was achieved for over 4 hours, 3.5 of which were at maximum vacuum of ~-25 inHg. The data from these pressure tests is displayed in Fig 5.15. With a proven method to hold pressure, full size payload testing could begin.

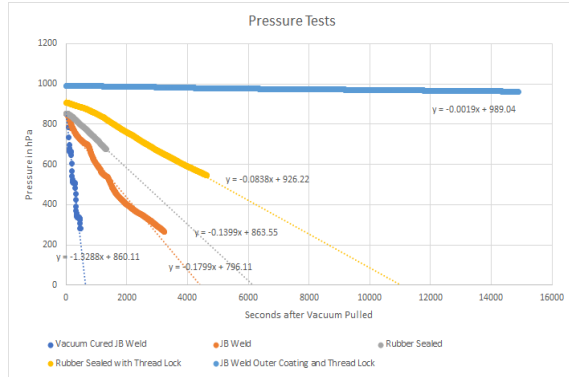


Fig. 5.18: Plots of pressure vs time to quantify pressure loss.

Scaling up from 4" x 2" diameter tube to 6" x 6" diameter tube proved difficult. Additional considerations were necessary to seal the central column, which was made of PETG and was not airtight. There were also issues with the dimensions of the column, which was designed around the assumption that the carbon fiber tubing had a height of exactly 6 inches. When the carbon fiber tubing arrived, it was 24" long and required cutting down to our specifications. Due to concerns with the carbon fiber dust particles shorting the electrical circuits of the campus machine shops' power tools, options for cutting the tubing were limited to a chop saw with a circular, abrasive blade. Unfortunately, the blade was not large enough in diameter to cut completely through the tubing, and multiple passes were necessary during cutting, causing an uneven surface in the cuts. The necessary removal of material to flatten the uneven cuts caused the overall height to become less than 6", so when the tubing was adhered to its end pieces, the central column did not line up perfectly in height with the sides. The uneven surfaces made it impossible to seal with the O rings, because excessive downward pressure

applied by the thread-on window cap would compromise the glass window. Subsequent attempts to fix this problem proved to be time consuming and fruitless, and with the deadline rapidly approaching, a decision was made to forgo attempts to seal the entire payload and instead focus on sealing of the individual test tubes. The reason behind sealing the system was to keep the nitrogen and carbon dioxide from being pulled out of the algae and starving them of necessary nutrients. The low surface area of the test tube dropped the pressure forces to negligible and vacuum chamber testing of this method proved to be successful. The only downside was the loss of convective heating within the payload. This wasn't necessary, however, because the items deemed 'temperature critical', the algae and the battery, were already being heated conductively. With this solution, although the goal of a fully sealed system was not achieved, the experiment was able to continue unaffected.



Fig. 5.19: Pressurized test tubes on flight day

Window Transmissibility

Material selection for the solar radiation transmitting window was based on

transmittance of the desired UV wavelengths. A mercury lamp was used to emit a specific wavelength of 254 nm. These emitted wavelengths were received by a spectrophotometer approximately 1” away from the emitting lamp. A control reading was gathered using air as the sole medium that the light had to pass through as shown in blue in figure 5.20. Subsequent trials were conducted using standard annealed glass, fused quartz, and acrylic plastic. It was found that the fused quartz allowed for the highest transmittance of the 254 nm UVC radiation, as hypothesized.

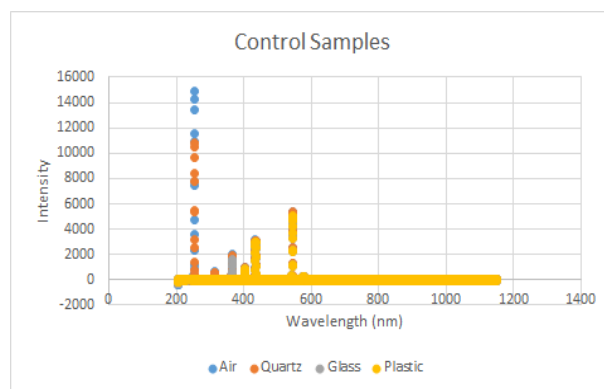


Fig. 5.20 Spectrophotometer Intensity Readings for Select Window Materials and a control (air)

Electronics

The electronics underwent multiple tests to prepare the payload for flight. The first was to simply let the Arduino run off the battery for 3 hours and gather data. This test was to confirm the chosen battery could last the duration of the flight under standard temperature and pressure conditions. Shorter length tests were run to confirm the sensors were running correctly before the longer test was conducted.

The next test was the shake test. The internals were placed inside the payload and shaken for 60 seconds. The idea was to make sure all the connections were secure for any turbulence during flight. Initial runs of this test revealed some issues with the wiring method chosen during the design process. Unexplainable electronics failures occurred after other tests, seemingly at random, and the shake test was deemed to be the culprit. Further investigation showed that, although the soldering of wires into the perf board provided a semi-permanent solution that was relatively secure, it was likely incapable of maintaining a solid electrical connection during high amounts of turbulence. Many of the wire connections were prone to becoming loose within the solder, and the wires going into the Arduino board were also prone to working themselves out of the Dupont female end connectors. Proper diagnosis of this problem took time; sometimes the electronics would work fine, and sometimes no data was gathered. A relatively secure solution was achieved by soldering the Arduino wires to sets of pins and utilizing heat shrink to insulate the connection. These sets of pins were then superglued into the Arduino board in their proper electronic configuration. The adhesion of the plastic insulation of the pin sets to the plastic Dupont adaptors provided a much more secure connection. However, the payload still suffered electrical issues after subsequent shake tests. The decision was made to achieve the best electrical solution possible and

couple it with careful handling and multiple electrical tests right up until the time of launch.

Heat Transfer

The initial design called for a convective heating solution due to the plans to seal the external payload structure. When this was no longer deemed possible in the given time frame, the decision was made to switch from convective to conductive heating of the most critical experimental components: the battery and the algae samples. Three flexible electric heating pads were recycled from past projects. Two were placed on the algae and one was placed with the battery. Allowing the algae to freeze would add another variable to the post growth analysis, fundamentally changing our experiment. Additionally, if the battery was allowed to get too cold, the low temperatures would affect the reaction rate of the internal battery chemistry and diminish its ability to provide power to the Arduino mid-flight. With the heating pads placed on those two spots, conductive heating would keep them warm, even despite the loss of convective heating due to the near vacuum conditions at altitude.

To test the heating system a cold test was performed. The payload was placed in a cooler filled with dry ice with an ambient temperature of $\sim -60^{\circ}\text{C}$ for 3 hours. Initial tests were conducted when the payload had two layers of insulation on the outside, with a half layer on the inside walls. Upon retrieval, no negative effects were observed to either the battery or the algal specimens. The data from the SD card for this test is

visible in figure 5.21. The temperature stayed around the desired 15°C for the duration of the test.

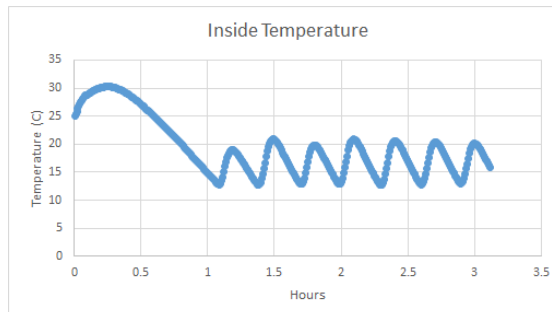


Fig. 5.21: Inside temperature during cold test

6) Flight Day

Three team members stayed at a hotel the night prior to scout the launch site and reduce travel time in the morning. This allowed for multiple electronics tests to be conducted with the goal of negating the effects of the faulty wiring scheme that were discovered during the testing phase of the electronics over the previous weeks. Tests were conducted on both battery and USB power reading to both the serial monitor in the Arduino integrated development environment (IDE) and the SD card. This was performed each time the payload's location changed to ensure that no wiring came loose during transportation. 2 Erlenmeyer flasks of the mother cultures were brought along, as well as the necessary equipment to properly measure out desired amounts of algae/media. Methods of cleaning and proper disposal of waste liquids were also brought along. Two 8mL samples of each

species were measured and placed into their respective test tubes. The tubes were then sealed with two applications of hot glue around the test tube cap/tube interface. This method proved effective for all but one sample, although it is still unknown whether the loss of fluid in the filtered AP sample was due to a pressure leak, the jolt of the payload upon impact with the ground, or simply a leak induced by payload walls making contact with the test tube cap. Further inspection and analysis of the post flight data led to a consensus that the leak was likely caused by the tight fit of the specimens within the payload.



Fig. 6.1: Early Morning Start

The payload was launched from Genoa, Colorado at 6:57 AM MT on August 1st, 2021.



Fig. 6.2: Top of the payload

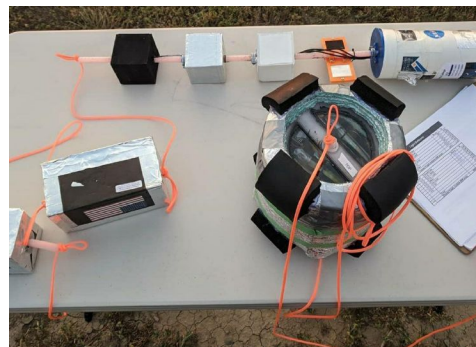


Fig. 6.3: Payloads on the flight string



Fig. 6.3: Assuming a "U" formation for launch

7) Data and Observations

Observations

Due to some unforeseen issues with the landing site, the team was unable to directly participate in payload recovery operations. Once the payload was retrieved by EOSS, the payload was given an immediate visual inspection. All the force dampeners were still attached and no noticeable dings in the insulation were observed. No cracks were observed in the window. The LED on the TSL2591 was off, indicating a problem with the electronics. The switch was still in the 'on' position, indicating a wiring issue. After

analysis of the time data, it was concluded that the cause of the wiring issue was the initial impact of the landing, although it is also possible that the payload was dragged by the parachute canopy after landing, since recovery operations took well over an hour. The payload was opened and a quick internal temperature was taken with a thermocouple. The internal temperature near the samples appeared to have equalized with the ambient temperature at $\sim 24^{\circ}\text{C}$. Further analysis of the temperature data from the sensors aboard indicated that overheating inside the payload was unlikely. Upon further inspection, the filtered AP test tube had lost some liquid and the insulation around it was damp. Compared to the other test tubes, approximately 2-4 ml of liquid was lost. With no signs of cracking, it was concluded that the tight fit of the samples within the payload may have induced some force on the side of the test tube cap, causing a small leak in the seal. The team then split to continue the post flight protocol. Team 1 took the algae to get it inoculated, while team 2 continued into sensor data analysis and diagnosis of the electrical issue. The battery voltage was measured to be $\sim 11.81\text{V}$, which supported the hypothesis of a wiring issue causing the loss of power.

Sensor Data

With an inconclusive answer on whether the electronics were working, the data on the SD card was analysed. The data was collected in two time segments, a 2.15 hours section and an 8 minute section. A

comparison to the flight data available from EOSS confirmed that this time period encompassed the entire flight, and that the break in the data occurred right about when the payload was said to have landed on the ground. This was confirmed when the BMP180 data was plotted, and further supported the hypothesis of impact causing the wiring issues.

Figure 7.1 shows the pressure dropped to 1455 Pa, then returned to where it started, indicating that the payload had returned to the ground before it stopped recording. It was concluded that the impact is likely what stopped the data recording. The BMP180 also recorded an approximate altitude. Plotting that and assuming some error, the data also cuts off at the same height. This is shown in figure 7.2.

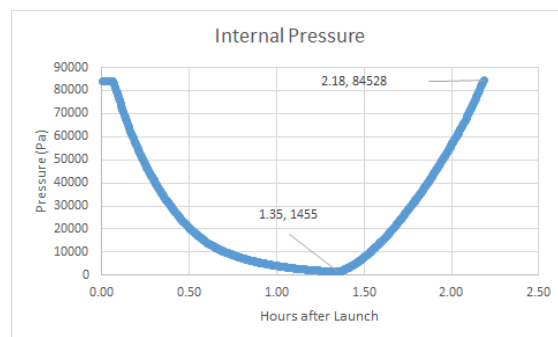


Fig. 7.1: Internal pressure during flight

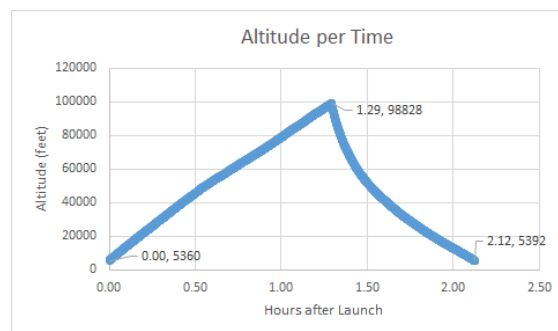


Fig. 7.2: Altitude change during flight

One of the biggest concerns was keeping the algae warm inside the payload. The graph below (figure 7.3) shows the payload managed to maintain $\sim 15^{\circ}\text{C}$, indicating that the heating system had performed as intended.

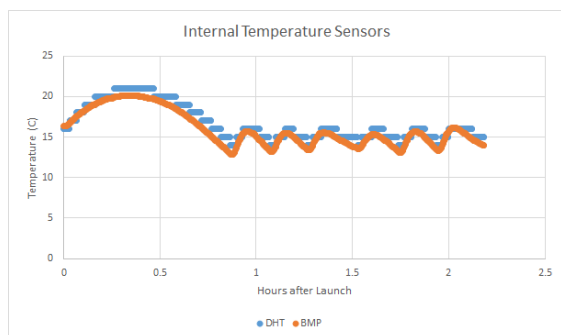


Fig. 7.3 Internal temperature sensors during flight

A trendline was applied to the TSL2591 data to aid in data analysis. The TSL2591 data was extremely scattered and thus analysis of light exposure compared to altitude proved difficult. However, this sensor did yield the lux at our max altitude which can be used in quantifying UVC irradiance. Originally, it was hypothesized that an increase in overall light exposure (higher lux readings) would be observed at maximum altitude due to decreased atmospheric scattering, and that it would decrease again as it returned to the ground. The opposite was observed; more light was observed on the ground than at the max altitude. Further deliberation led to the conclusion that due to the launch occurring at 7 am, the incident angle of sunlight on the payload window was not ideal. The sun was low on the horizon, and as the balloon gained altitude, the expected change in incident angle of sunlight (0° being normal to the payload window) was slowed due to the rapid change in altitude. This reduced

the overall light exposure and resulted in lower lux readings. This effect was likely exacerbated by the extra insulation and padding that was applied to the window cap. Although the initial low light conditions were anticipated, it was originally assumed that the change in relative position of the sun in the sky during flight would be sufficient to allow for a favorable incident angle of light upon the window as the payload arrived at maximum altitude. Another part of the graph that supports this hypothesis is the end points. The first lux reading was smaller than the last lux reading, which could be explained by the changing incident angle of sunlight on the payload as the day progressed. When the payload landed, just over two hours had passed since launch and the sun was higher in the sky, resulting in a more favorable incident angle with the payload window than at launch. It is hypothesized that this issue severely reduced the amount of UVC exposure allowed to reach the samples.

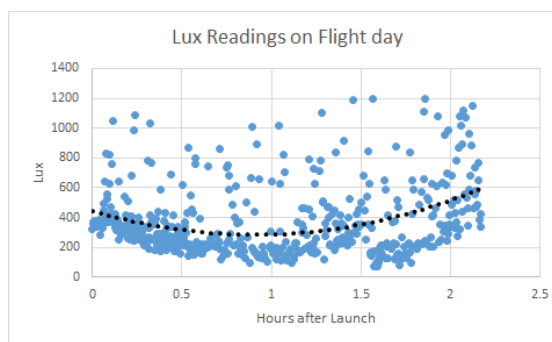


Fig. 7.4 : Lux reading on flight day

Algae Data

8 algae trials (4 from each algae species, Fig 7.5) were conducted post flight:

filtered from UVC light, unfiltered, controlled, and UVC treated in the lab.



Fig. 7.5: Post flight algae trials

The first 2 trials were those inside of the payload. The UVC treated trial consisted of 2 8mL samples subjected to 5 minutes of UVC radiation from a 25W bulb positioned approximately 1” above the quartz tubes as seen in figure 7.6.



Fig 7.6 UVC Trial

Temperature and pH

The pH and temperature values remained relatively constant throughout the growth

period with AP samples ranging from 10.5 to 11 pH and CV samples ranging from 9.5 to 10. Temperature ranged from 22.8°C to 24.2°C, which is slightly under nominal temperature for both species.

Biomass

The biomass yield test did not provide the expected results (see Fig. 7.7). For both AP and CV, there was no difference between UVC filtered and unfiltered. The AP control biomass was by far the highest at 0.3 gdcw as compared to 0.17 (Filtered and Unfiltered). The CV control biomass slightly underperformed as compared to filtered and unfiltered at 0.05 gdcw and 0.06 gdcw, respectively. The UVC biomass yields were, surprisingly, only slightly lower than the other tests; 0.16 gdcw for AP and 0.04 gdcw for CV.

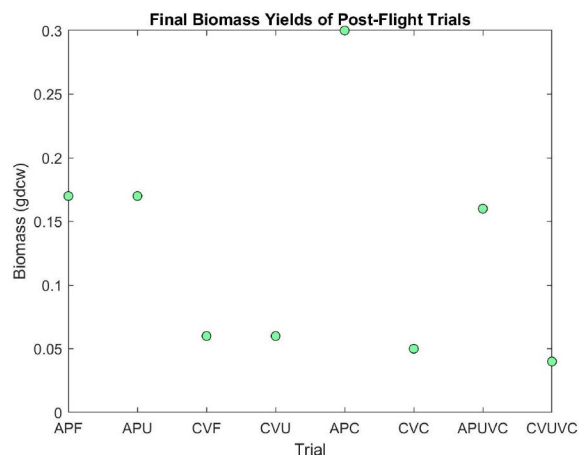


Fig. 7.7: Biomass Yield

The data for optical density is plotted in figure 7.8. This data is easier to analyze once converted to concentration, which can be found on page 29.

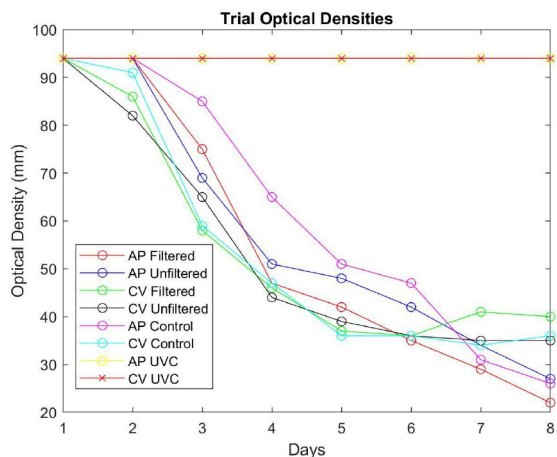


Fig. 7.8: Optical densities

Microscopy Preflight



Fig. 7.9: Preflight AP

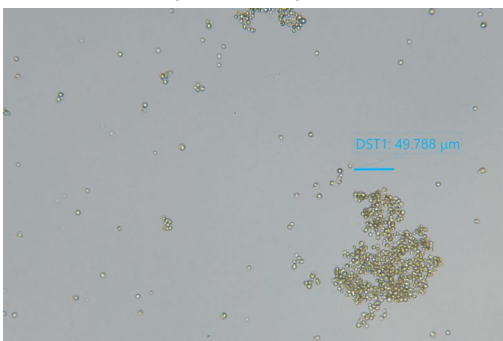


Fig. 7.10: Preflight CV

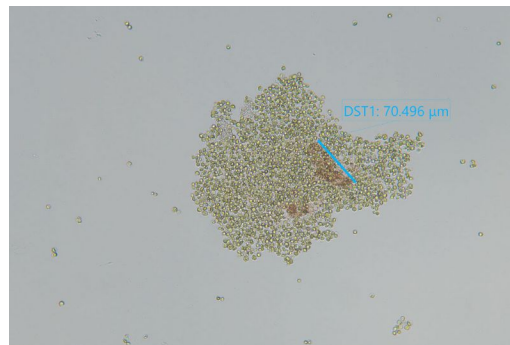


Fig. 7.11: Preflight CV (cont.)

From the preflight pictures the algae looks relatively normal and healthy with only a couple sections of the CV flocculation displaying high concentrations of carotenoids.

Microscopy Postflight

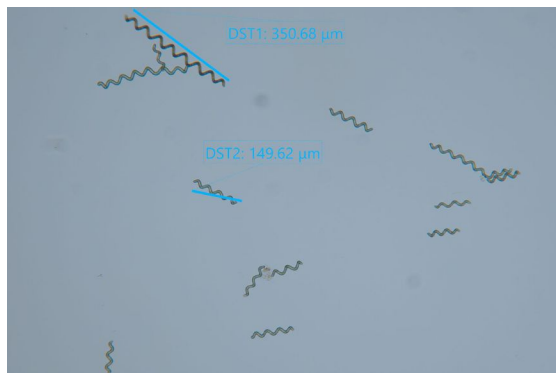


Fig. 7.12: AP Filtered (day 1)

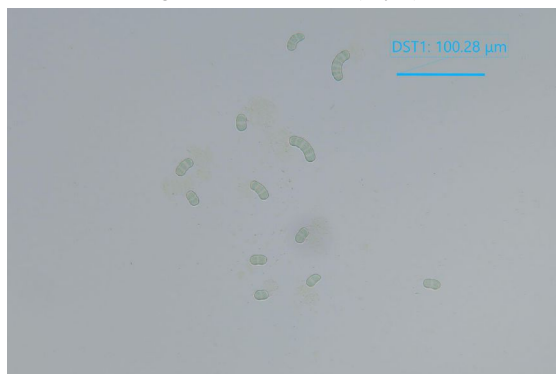


Fig. 7.13: AP Unfiltered (day 1)

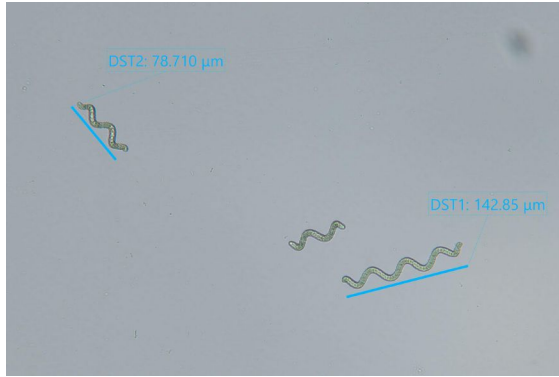


Fig. 7.14: AP Control (day 1)

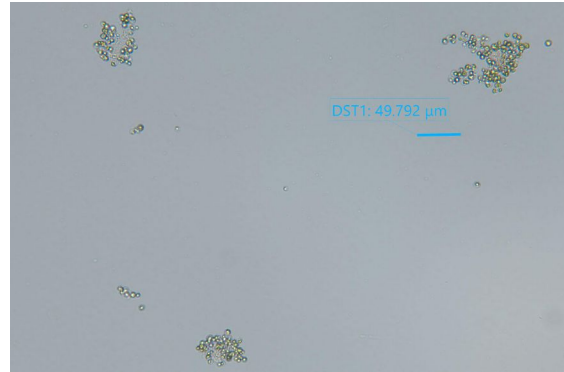


Fig. 7.18: CV Control (day 1)

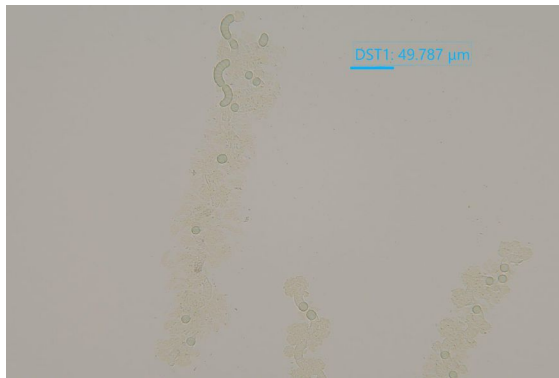


Fig. 7.15: AP UVC (day 1)

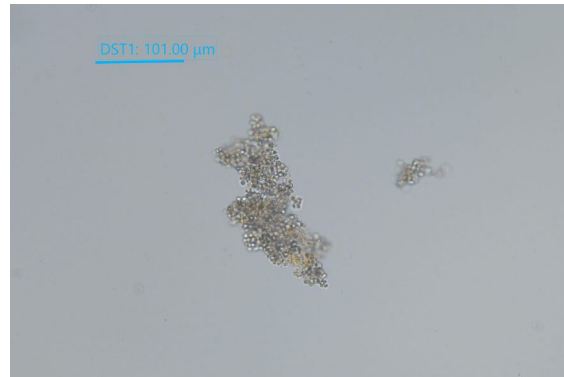


Fig. 7.19: CV UVC (day 3)

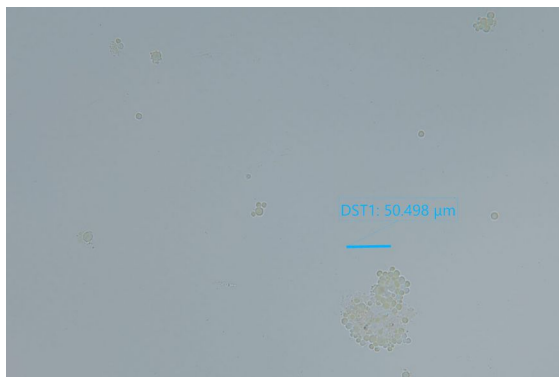


Fig. 7.16: CV Filtered (day 1)

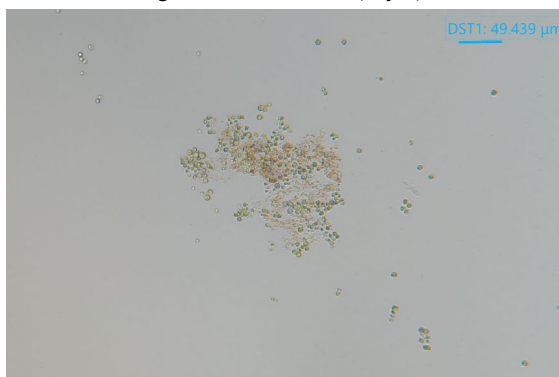


Fig. 7.17: CV Unfiltered (day 1)

The maximum irradiance value at our maximum elevation of ~99k ft was 1,101.412 lux. Using the method as outlined in the *Quantifying UVC* section, the calculated UVC intensity was 1.1658 W/m². This was much lower than expected, likely due to the angle of incidence. Even with a longer exposure time, this amount of UVC light is much less than the study cited on page 10 of this report (~155 W/m²) [14].

All postflight microscopy pictures shown here were taken in the early stages of growth in order to identify direct morphological changes from flight. The filtered and controlled trials appear relatively normal and healthy. The unfiltered AP trial shows some unusual behavior with abnormally small

hormogonium, lack of large trichomes, and widespread ‘pools’ of cytoplasm. These large pools of cytoplasm are hypothesized to be caused by a literal dissolving of cells from high energy radiation. These same characteristics are amplified in the AP UVC trial. The unfiltered CV trial shows large areas of high carotenoid concentration. However, the cells in this trial generally seem unaffected due to their retention of color and cell walls. The CV UVC trial shows massive cell casualties as evidenced by the lack of photosynthetic pigments and desiccation. These morphological changes are in line with the initial experiment hypothesis.

The post-flight secchi stick measurements were used to determine concentration vs time to quantify growth. Starting with AP, the data revealed almost identical growth between both flight samples and the ground control. The sample that was exposed to a direct UVC lightbulb saw no growth. It was determined that the AP samples were exposed to little to no UVC during the flight.

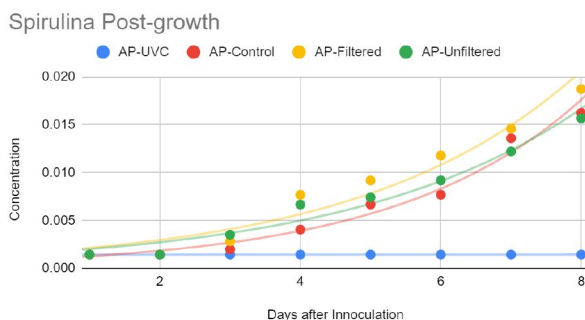


Fig. 7.20: AP concentration vs time

The CV showed similar results. Instead of fully exponential growth, the CV started to

level off, indicating a harvest was needed soon. This growth was seen between both flight samples and the growth control. The UVC exposed sample appeared to have died as well. In the later half of the experiment, some growth was seen from that sample but it is hypothesized that secchi stick cross-contamination may be responsible for the late growth in this trial. Again the unfiltered sample closely matches the control samples rather than the UVC bulb exposed, showing little to no UVC exposure on flight day.

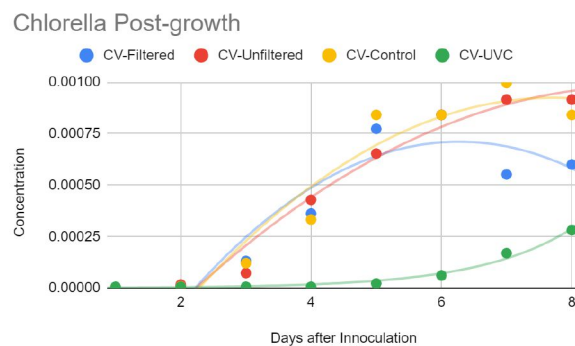


Fig. 7.21: CV concentration vs time

8) Budget, Management, and Schedule

Management

Throughout the duration of this project, each team member assisted in the design and manufacturing of each subsystem. However, individuals did take a “focus” as described in the following table:

Subsystem	Team Member
Circuitry and Arduino	Karla Rueda Perez
Phycology	Jacob Julius
Structural	Justin Raffa and Richard Nash

Schedule

Week	Task
1	Brainstorming and ordering parts
2	Preliminary design review, CAD designs, and Arduino coding
3	Begin 3D printing and electronics assembly
4	Begin algae growth experiments and manufacturing prototypes
5	Critical design review and pressure testing prototypes
6	Pressure testing prototypes
7	Electronics and payload assembly
8	Cold testing and pressure testing

9	Structural testing and troubleshooting electronics
10	Launch readiness review and launch

Financial and Mass Budgets

The team successfully stayed under the budget and mass constraints. The allotted mass was increased from 1500g to 1600g upon request.

Subsystem	Mass (g)
Electronics	336
Structural	1066
Algae	119
Total	1521

Subsystem	Part	Distributor	Cost (\$)	Quantity
Structural	Carbon Fiber Tubing	DragonPlate	\$197.15	1
	PETG Filament	Amazon	\$22.00	1
	PETG Filament	Donated	\$0.00	3
	Quartz Sheet	Technical Glass Products	\$132.70	1
	Pipe Insulation	Donated	\$0.00	1
	HVAC Insulation	Donated	\$0.00	1
	Space Blanket	Donated	\$0.00	1
	Zip Tie	Amazon	\$12.00	1
	Polyethylene Tubing	Donated	\$0.00	1
	JB Weld Original	Amazon	\$15.00	1
	JB Weld Original	Donated	\$0.00	2
	Loctite Plastic Bonder	Amazon	\$7.00	1
	Grommets	Amazon	\$20.00	1
	Mounting Washers	Home Depot	\$1.18	1
Electronics	Arduino Uno	Amazon	\$29.00	1
	SD Shield	Amazon	\$8.50	1
	DHT11	Donated	\$0.00	1
	BMP180	Donated	\$0.00	1
	TSL12591	Amazon	\$8.00	1
	Relay	Amazon	\$5.00	1
	Heating pad	Donated	\$0.00	3
	Voltage Regulator	Amazon	\$8.00	1
	220 UF 25V Capacitors	Amazon	\$6.00	1
	12V 4000mAh Battery	Folk Battery	\$15.00	2
	SI1145 (Inconsistent)	Amazon	\$16.00	1
	Geiger Counter (Broke)	Amazon	\$46.00	1
	BMP 390 (Incompatible)	Amazon	\$16.00	1
	Spirulina Sample	Amazon	\$26.00	1
Algae	Chlorella Sample	Amazon	\$26.00	1
	Media for Spirulina 5L Kit	Algae Research and Supply	\$20.00	1
	Fresh Water Media 5L Kit	Algae Research and Supply	\$25.00	1
	Sechi Sticks	Donated	\$0.00	2
	Plastic Test Tubes (50)	Amazon	\$8.00	1
	Quartz Test Tubes	Technical Glass Products	\$17.85	2
	Neoprene Spacers	Donated	\$0.00	1
	Aerator	Amazon	\$21.00	1
	Algae Storage Tanks	Donated	\$0.00	1
	Growth Lights	Donated	\$0.00	1
	Misc Lab Equipment	Donated	\$0.00	1
	Erlenmeyer Flask Set, 5 Sizes	Amazon	\$20.00	2
	125 ml Erlenmeyer Flask	Chemistry Stock Room CSU	\$6.79	6
	Rubber Stoppers	Amazon	\$13.00	1
Flight Day	Hotel Room	Econo Lodge	\$121.00	1

Total	\$955.97
-------	----------

9) Conclusion

Overall, this experiment was deemed a success. All systems remained functional throughout the duration of the flight. The electronics were able to successfully regulate temperature and all sensors gathered data for the entire flight. The internal and external structural systems were able to protect the window, algae, and electronics against the impact force and net kinetic forces. Lastly, although the light sensor data was relatively inconclusive, the post flight morphological analysis appears to support the original hypothesis for the

effects of UVC radiation on the samples. In contrast, the growth kinetics analysis did not support the initial hypothesis as the data showed significant growth in the unfiltered samples.

Unfortunately, one major flaw in the design of the payload window was realized after the flight. The incident angle of light rays on the payload window was not considered and thus the majority of the radiation did not come in contact with the quartz tubes due to their centered position in the payload. The unfiltered plastic tubes received more radiation due to their placement near the edges of the window. The TSL2591 sensor was positioned under the PETG “bridge” and thus the irradiance readings were scattered, possibly due to the rotation of the payload. This was likely the reason behind the unexpected growth kinetics analysis results. Upon reflection, this issue could be fixed by altering the window design from flat to a dome structure, which would allow for increased radiation from a wider range of incident angles.

Message to Next Year

If your project is to use biological samples, be sure to look up environmental and human toxicity prior to choosing the species. If your project is to focus on radiation effects, do not forget to take into account the position of the sun/incident angle of sunlight at the time of launch. Do not be afraid to make mistakes; 90% of ours ended up having relatively simple fixes to them, but we lost a lot of time

sitting around thinking things through for fear of making these mistakes instead of doing and fixing. Finally, push the boundaries with the goals of the project! You will gain much more out of the experience by challenging yourself and incorporating unconventional ideas.

Acknowledgments

Mathew Huber at Algae Research and Supply - Tips on algae growth techniques and troubleshooting

Kathi Dougherty, KDD Fused Glass -

Tools & insight into glass cutting

Dr. Azer Yalin - Resources and project design/schedule guidance

James Sipich - Guidance and aid

throughout various project areas

Mech Department and the Idea2Product

lab at CSU - The tools to print and

manufacture our payload

References

1. M. Johnson, "Better Life Support Systems for Space Travel," *NASA*, April 26, 2019. [online], Available: https://www.nasa.gov/mission_pages/station/research/news/photobioreactor-better-life-support
2. V. Kumar, M. Nanda, H.C. Joshi, A. Singh, S. Sharma, and M. Verma, "Production of Biodiesel and Bioethanol Using Algal Biomass Harvested from Fresh Water River," *Science Direct*, October 5, 2017. [online], Available: <https://www.sciencedirect.com/science/article/abs/pii/S0960148117309771?via%3Dihub>
3. M. Molazadeh, H. Ahmadzadeh, H. Pourianfar, S. Lyon, and P. Henrique Rampelotto, "The Use of Microalgae for Coupling Wastewater Treatment with CO₂ Biofixation," *Frontiers in Bioengineering and Biotechnology*, March 2019, [Online serial]. Available: <https://www.frontiersin.org/articles/10.3389/fbioe.2019.00042/full>
4. S. Mathewson, "Algae 'Bioreactor' on Space Station Could Make Oxygen, Food for Astronauts," *Space.com*, May 8, 2019. [online], Available: <https://www.space.com/space-station-algae-experiment-fresh-air.html>
5. International Agency for Research on Cancer, "Solar and Ultraviolet Radiation," *NCBI*, 2012, [online serial]. Available: <https://www.ncbi.nlm.nih.gov/books/NBK304366/>
6. R. E. Lee, *Phycology (5th Edition)*. Cambridge University Press, 2018
7. C. Jung, S. Braune, P. Waldeck, J. H. Küpper, I. Petrick, and F. Jung, "Morphology and Growth of *Arthrospira Platensis* during Cultivation in a Flat-Type Bioreactor", *MDPI*, June, 202, [online serial]. Available: <https://www.mdpi.com/2075-1729/11/6/536/htm>
8. A. Pandey, J. Chang, C. R. Soccol, D. Lee, Y. Chisti, *Biofuels from*

- Algae*, 2nd ed. Elsevier, 2019.
[E-book]. Available:
<https://www.sciencedirect.com/book/9780444641922/biofuels-from-algae#book-description>
9. “Amount of Protein in Spirulina”, *Diet & Fitness Today*, n.d, [online]. Available:
<http://www.dietandfitnesstoday.com/protein-in-spirulina.php>
 10. J. Paniagua-Michel, *Handbook of Marine Microalgae*, Elsevier, 2015. [E-book]. Available:
<https://www.sciencedirect.com/book/9780128007761/handbook-of-marine-microalgae#book-info>
 11. K. Bišová and V. Zachleder, “Cell-Cycle Regulation in Green Algae Dividing by Multiple Fission,” *Journal of Experimental Botany- Oxford Academic*, 17 January, 2014. [online serial]. Available:
<https://academic.oup.com/jxb/article/65/10/2585/573549>
 12. C. U. Aguoru and P.O. Okibe, “Content and Composition of Lipid Produced by *Chlorella Vulgaris* for Biodiesel Production,” *National Research Institute for Chemical Technology*, 2015. [online serial]. Available:
<https://core.ac.uk/download/pdf/234687246.pdf>
 13. J. K. Johnson and J. T. Yates, *Molecular Physical Chemistry for Engineers (1st edition)*. University Science Books, 2007.
 14. T. Dai, M. S. Vrahas, C. K. Murray, and M. R. Hamblin, “Ultraviolet C Irradiation: An Alternative Antimicrobial Approach to Localized Infections?,” *NCBI*, 2012. [online serial]. Available:
<https://www.ncbi.nlm.nih.gov/pmc/articles/PMC3292282/>
 15. “Desorption,” *Wikipedia*, 21 July, 2021, [online]. Available:
<https://en.wikipedia.org/wiki/Desorption>
 16. “Properties of Carbon Fiber,” *Clearwater Composites*, n.d, [online]. Available:
<https://www.clearwatercomposites.com/resources/properties-of-carbon-fiber/>
 17. “PETG,” *Dielectric Manufacturing*, 27 February, 2019, [online]. Available:
<https://dielectricmfg.com/knowledge-base/petg/>
 18. T. Rodgers, “Everything You Need to Know About Polylactic Acid (PLA),” *Creative Mechanisms*, 7 October, 2019, [online]. Available:
<https://www.creativemechanisms.com/blog/learn-about-poly-lactic-acid-pla-prototypes>
 19. “ABS (Acrylonitrile-Butadiene-Styrene),” *Dielectric Manufacturing*, 27 February, 2019, [online]. Available:
<https://dielectricmfg.com/knowledge-base/abs/>
 20. “Fused Silica / Fused Quartz,” *ESCO Optics*, n.d, [online]. Available:
<https://escooptics.com/pages/materials-fused-silica-quartz#:~:text=UV%20fused%20silica%20provides%20>

- [20excellent.lasers%20and%20challenging%20environmental%20conditions.](#)
21. V. Smil, “Our Best Lamps Still Can’t Equal the Luminosity of the Sun,” *IEEE Spectrum*, 27 March, 2019, [online]. Available: <https://spectrum.ieee.org/our-best-lamps-still-cant-equal-the-luminosity-of-the-sun>
 22. “Petalomonas,” *Wikipedia*, 27 July, 2021, [online]. Available: <https://en.wikipedia.org/wiki/Petalomonas>
 23. Advanced Glass Industries, “Pressure Window Design” *Advancedglass.net*, [online], Available: https://www.advancedglass.net/Images_Content/Site1/Files/Pages/PressureWindows.pdf
 24. C. Boucher, “What is the Coefficient of Thermal Expansion? How to Measure it?,” *Thermtest Instruments*, 30 October, 2019, [online]. Available: <https://thermtest.com/what-is-coefficient-of-thermal-expansion-how-to-measure-it>
 25. “About Pitch Based Carbon Fiber “GRANOC” / Low Thermal Expansion,” *Nippon Graphite Fiber Corporation*. N.d, [online]. Available: https://www.ngfworld.com/en/fiber/low_thermal_expansion.html